 https://doi.org/10.3311/PPci.22964

Periodica Polytechnica Civil Engineering, 68(2), pp. 364–374, 2024

Investigations on the Effects of Rail Longitudinal Forces in Train-Track Dynamic Interaction

Amirhesam Taghipour[1], Jabbar Ali Zakeri[1*], Seyed Ali Mosayebi[1]

[1] School of Railway Engineering, Iran University of Science and Technology, Tehran, 1684613114, Iran
[*] Corresponding author, e-mail: zakeri@iust.ac.ir

Received: 10 July 2023, Accepted: 21 September 2023, Published online: 26 October 2023

Abstract

Nowadays, attention to railways has been increased as one of the important transportation methods. Various factors can cause longitudinal forces on the railway tracks, so the most important factors are the temperature changes due to the rail contraction and expansion (thermal forces), train braking system forces and acceleration, etc. Increasing longitudinal force can lead to buckling phenomena in railway tracks. In this paper, the effects of tensile and compressive longitudinal forces on the parameters of rail, sleeper, and ballast layers under vertical moving loads are investigated by using the finite element method. In this regard, by performing sensitivity analyses for different values of longitudinal forces and train speeds dynamic responses (displacement, velocity, and acceleration) of railway track components like rail, sleeper, and ballast have been studied. The results show that increasing the values of longitudinal axial force from –2000 [kN] up to 2000 [kN] as well as increasing the train speed from 10 [m/s] (36 [km/h]) up to 100 [m/s] (360 [km/h]) increases the rail displacement and velocity in the range of 25% up to 37% also the rail acceleration in the range of 9% up to 14%. The velocity and acceleration of the sleeper also the ballast velocity increase in the range of 24% up to 30% and 7% up to 9%, respectively, by increasing the speed of the train from 10 [m/s] (36 [km/h]) to 100 [m/s] (360 [km/h]) in all three modes without applying axial force, considering compressive and tensile one in the train-track interaction system.

Keywords

ballasted railway tracks, train-track interaction system, thermal forces, finite element method, train speed

1 Introduction

Due to the dynamic nature of the train-track interaction problem, researchers have interest to analyze the dynamic effects of the different forces on the railway tracks [1]. One of the main considerations in analyzing the dynamic behavior of rail is the evaluation of the stiffness matrix of the system as it changes constantly over [2]. Since the past, different methods have been developed for the dynamic analysis of the train-track interaction used by researchers. Over the years the researchers have taken more complete assumptions to resolve the issue, from the moving load to more complete models of the moving vehicle [3]. Also besides, the track and infrastructure system models have been considered by researchers from simple models such as beam on an elastic foundation to more accurate models today [4]. There are various methods used to solve the train-track interaction problems, such as closed-loop solutions (Fourier transforms), and numerical solutions (the finite element method). Xu et al. [5] analyzed the effect of lateral and local rail displacement on the train–track dynamic interaction in high-speed railway tracks. In this study, they assumed the laterally and locally deformed rail as a curved rail and simulated the train–track interaction with lateral and local rail deformation using a reduced beam model with required modifications to provide the curved rail. In the finite element method due to the specified model, degrees of freedom have clarified and the related equations of motions of the model also have been obtained. Then by solving these equations of motions, the expected analysis is performed. It should be noted that in the mentioned method because of the varying load of the vehicle, the stiffness matrix in each time step has been changed that research are dealing with a new stiffness matrix or new equations of motions in the system [6, 7].

In the analysis of train-track interaction problems for the moving load of the vehicle, the load vector is required to be modified at any time step to enter the correct position

Cite this article as: Taghipour, A., Zakeri, J. A., Mosayebi, S. A. "Investigations on the Effects of Rail Longitudinal Forces in Train-track Dynamic Interaction", Periodica Polytechnica Civil Engineering, 68(2), pp. 364–374, 2024. https://doi.org/10.3311/PPci.22964

of the load at any moment into the related calculations [8]. Also, due to the contact stiffness between the vehicle and the rails in considering the effect of vehicle load and its mass and stiffness, the analysis is required to correct the stiffness and damping matrices and also the mass matrices according to the motion of the vehicle at each time step [9]. In this analysis, also it is necessary to create artificial boundary conditions at the end of modeled rail. Fryba investigated the behavior of railway track as a beam on an elastic foundation under moving loads [10]. Hou et al. [11] considered an asymmetrical finite element method from the track and train system. In their study, the vehicle as a two-dimensional wagon with two-axle bogies with 10 degrees of freedom and rail as a continuous beam were considered. The results of the various components of the track were then presented as time history graphs of displacement, velocity, and acceleration. Zhai and Sun [12] arranged complete modeling to understand how train-track interaction is occurred. In their research, they divided the model into two subsystems of vehicle and track, as well as a three-layers-model for the track subsystem including rail, sleeper, ballast is assumed. In this research, rail is modeled as an infinite Euler-Bernoulli beam supported on a discrete-continuous elastic foundation. Wang et al. [13] evaluated the coupled effect on the running safety between elastic railway tracks and longitudinal stimulation of Long Heavy Haul Train (LHHT) using a train-track dynamic interaction model based on connection substructure theory. Zakeri and Xia [14] applied a two-dimensional finite element model to solve the dynamic train-track interaction problem. They used a combination of finite elements and two infinite elements to reduce the effects of boundary conditions on the dynamic response of the track and train. Zakeri et al. [15] investigated the effect of partially and unsupported sleepers on the rail's vertical displacement via a numerical analysis and under varied circumstances. In this research, and Euler-Bernoulli beam was used for a railway track model on discrete elastic supports as a system with connected mass, spring, and damper. Alkaissi [16] generated a combined 3D finite element model to simulate a railway track system with a ballast foundation that could better anticipate the train-induced vibrations and obtain dynamic responses of the train-track interaction system. Liu et al. [17] suggested connecting the two calibrated FEM (finite element model) and DEM (discrete element model) models to create a more realistic ballasted railway track model for predicting the dynamic responses of the train-track system.

In this research, the effects of tensile and compressive longitudinal forces on the parameters of rail, sleeper, and ballast layers under vertical moving loads have been investigated by using the finite element method. In this regard, by performing sensitivity analyses for different values of longitudinal forces and train speeds, parameters of railway track components have been studied as time history graphs.

2 Train-track model

In this paper, the ballasted railway track including rail, sleeper and ballast layers was simulated as a three-layer mass-spring model and also the moving vehicle was modeled as a two-dimensional car body with two-axle bogies and four wheel-sets with total 10 degrees of freedom. The numerical simulation is used in this research via MATLAB coding software [18] based on the finite element method. For analyzing the model, the Wilson-Theta numerical method was utilized, and sensitivity analyses were done based on train speed changes from 36 up to 360 km/h for various models with and without applying longitudinal compressive and tensile forces. Also, the results achieved in this research are compared with the results of other numerical results. The model of the track and the moving vehicle can be seen in Fig. 1. In this paper, the track model was studied in three states without considering longitudinal force, considering compressive longitudinal force (C) (positive value [+]) and also considering tensile longitudinal force (T) (negative value [–]) as shown in Fig. 1.

The general equations of motion for a multiple-degree of freedom discrete system with n degrees of freedom are written as [19–21]:

$$[M_T]\{\ddot{X}\}+[C_T]\{\dot{X}\}+[K_T]\{X\}=\{F\} \tag{1}$$

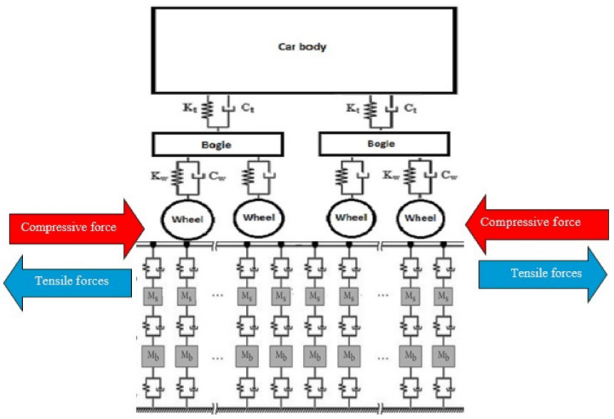

Fig. 1 Track and moving vehicle model without and with considering compressive longitudinal force(C) (positive value [+]) and tensile longitudinal force (T) (negative value [–])

Parameters of the mentioned equation are presented in Table 1.

Since the purpose of this study is to investigate the effect of the longitudinal force, the Rail New Stiffness Matrix $[K_{Rail(New)}]$ will be given below by considering the longitudinal axial force effect:

$$\left[K_{GSM}\right] = P\begin{bmatrix} \frac{6}{5L} & -\frac{1}{10} & -\frac{6}{5L} & -\frac{1}{10} \\ -\frac{1}{10} & \frac{2L}{15} & \frac{1}{10} & -\frac{L}{30} \\ -\frac{6}{5L} & \frac{1}{10} & \frac{6}{5L} & \frac{1}{10} \\ -\frac{1}{10} & -\frac{L}{30} & \frac{1}{10} & \frac{2L}{15} \end{bmatrix}. \tag{2}$$

$$\left[K_{Rail(New)}\right] = EI\begin{bmatrix} \frac{12}{L^3} & -\frac{6}{L^2} & -\frac{12}{L^3} & -\frac{6}{L^2} \\ -\frac{6}{L^2} & \frac{4}{L} & \frac{6}{L^2} & \frac{2}{L} \\ -\frac{12}{L^3} & \frac{6}{L^2} & \frac{12}{L^3} & \frac{6}{L^2} \\ -\frac{6}{L^2} & \frac{2}{L} & \frac{6}{L^2} & \frac{2}{L} \end{bmatrix} - P\begin{bmatrix} \frac{6}{5\mathrm{L}} & -\frac{1}{10} & -\frac{6}{5\mathrm{L}} & -\frac{1}{10} \\ -\frac{1}{10} & \frac{2\mathrm{L}}{15} & \frac{1}{10} & -\frac{\mathrm{L}}{30} \\ -\frac{6}{5\mathrm{L}} & \frac{1}{10} & \frac{6}{5\mathrm{L}} & \frac{1}{10} \\ -\frac{1}{10} & -\frac{\mathrm{L}}{30} & \frac{1}{10} & \frac{2\mathrm{L}}{15} \end{bmatrix} \tag{3}$$

In these Matrices, parameters of E, I, L, and P are the modulus of elasticity, moment of inertia of the beam element, the length of the element and the longitudinal axial force in the form of tensile and compressive force, respectively. Also, the form of the stiffness matrix for both railway track and train model will be as follows (Eq. (4)):

$$\left[K_T\right] = \begin{bmatrix} K_C & K_{C/W} & 0 & 0 & 0 \\ K_{W/C} & K_W & K_{W/Rn} & 0 & 0 \\ 0 & |K_{Rn/W}| & K_{Rn} & |K_{Rn/S}| & 0 \\ 0 & 0 & K_{S/Rn} & K_S & K_{S/B} \\ 0 & 0 & 0 & K_{B/S} & K_B \end{bmatrix}. \tag{4}$$

In Eq. (4). K_C and K_W = carbody and wheel stiffness matrix; $K_{C/W}$ and $K_{W/C}$ = car body-wheel and wheel-car body interaction stiffness matrix; $K_{W/Rn}$ and $K_{Rn/W}$ = wheel-Rail new and Rail new-wheel stiffness matrix; K_S = sleeper stiffness matrix; K_B = ballast stiffness matrix; $K_{S/B}$ and $K_{B/S}$ = sleeper-ballast and ballast-sleeper stiffness matrix; K_{Rn} = Rail new stiffness matrix; $K_{Rn/S}$ and $K_{S/Rn}$ = Rail new-sleeper and sleeper-Rail new stiffness matrix, respectively. The equations of motion for the railway track components are similar to the ones used in Zakeri et al. [22] and for the vehicle including car body, bogie and wheels are as Table 2.

In Table 2 M_C and J_C = mass and inertia of car body; M_{td} and J_{td} = mass and inertia of d bogie; M_{wp} = mass of p wheel; K_{td} and C_{td} = stiffness and damping matrix of d bogie; K_{wp} and C_{wp} = stiffness and damping matrix of p wheel, respectively [22].

Table 1 Parameters of Eq. (1)

Parameters	Descriptions	
$[M_T]$	Total mass matrix of the system	$[M_T]$: $[M_C] + [M_R]$
$[C_T]$	Total damping matrix of the system	$[C_T]$: $[C_C] + [C_R]$
$[K_T]$	Total stiffness matrix of the system	$[K_T]$: $[K_C] + [K_R]$
$\{\ddot{X}\}$	Acceleration vector of the train-track system	
$\{\dot{X}\}$	Velocity vector of the train-track system	
$\{X\}$	Displacement vector of the train-track system	
$\{F\}$	Externally applied force to the train-track system	
$[M_C]$	mass matrix of the vehicle	$[M_C]$: $[M_{Carbody}] + [M_{Bogie}] + [M_{Wheel}]$
$[M_R]$	mass matrix of the railway track	$[M_R]$: $[M_{Rail}] + [M_{Sleeper}] + [M_{Ballast}]$
$[C_C]$	damping matrix of the vehicle	$[C_C]$: $[C_{Carbody}] + [C_{Bogie}] + [C_{Wheel}]$
$[C_R]$	damping matrix of the railway track	$[C_R]$: $[C_{Rail}] + [C_{Sleeper}] + [C_{Ballast}]$
$[K_C]$	stiffness matrix of the vehicle	$[K_C]$: $[K_{Carbody}] + [K_{Bogie}] + [K_{Wheel}]$
$[K_R]$	stiffness matrix of the railway track	$[K_R]$: $[K_{Rail}] + [K_{Sleeper}] + [K_{Ballast}]$
$[K_{Rn}$[kN/m]]	Rail new stiffness matrix	$[K_{Rn}]$: $[K_{Rail}] - P \times [K_{GSM}]$
$[C_{Rail}]$	damping matrix of the Rail	$[C_{Rail}]$: $\alpha[M_{Rail}] + \beta[K_{Rn}]$
α	Rayleigh coefficient for mass matrix	α: 400 [–]
β	Rayleigh coefficient for rail new stiffness matrix	β: 4×10^{-7} [–]
$[K_{GSM}]$	Geometric Stiffness Matrix of the rail including longitudinal (axial) force (P) [kN/m]	

Table 2 derived equations of motion of moving vehicle

Vehicle components	Vehicle motion	Derived equations
Car body	Vertical motion (X_C)	$M_C\ddot{X}_C + \sum_{d=1}^{2} K_{td}\left(X_C - X_{td}\right) + \sum_{d=1}^{2} C_{td}\left(\dot{X}_C - \dot{X}_{td}\right) = 0$
	Rotational motion (φ_C)	$J_C\ddot{\varphi}_C + \sum_{d=1}^{2} K_{td}L_C\left(\varphi_C L_C \pm X_{td}\right) + \sum_{d=1}^{2} C_{td}L_C\left(\dot{\varphi}_C L_C \pm \dot{X}_{td}\right) = 0$
Bogie	Vertical motion of d bogie (X_{td})	$M_{td}\ddot{X}_{td} + K_{td}\left(X_{td} - X_C \pm \varphi_C L_C\right) + C_{td}\left(\dot{X}_{td} - \dot{X}_C \pm \dot{\varphi}_C L_C\right) + \sum_{d=1}^{2} K_{wp}\left(X_{td} - X_{wp}\right) + \sum_{d=1}^{2} C_{wp}\left(\dot{X}_{td} - \dot{X}_{wp}\right) = 0$
	Rotational motion of d bogie (φ_{td})	$J_{td}\ddot{\varphi}_{td} + \sum_{d=1}^{2} K_{wp}L_t\left(\varphi_{td}L_t \pm X_{wp}\right) + \sum_{d=1}^{2} C_{wp}L_t\left(\dot{\varphi}_{td}L_t \pm \dot{X}_{wp}\right) = 0$
Wheel	Vertical motion of p wheel (X_{wp})	$M_{wp}\ddot{X}_{wp} + K_{wp}\left(X_{wp} - X_{td} \pm \varphi_{td}L_t\right) + C_{wp}\left(\dot{X}_{wp} - \dot{X}_{td} \pm \dot{\varphi}_{td}L_t\right) = 0$

The behavior of dynamic systems under the influence of time-dependent variations can be investigated based on ordinary differential equations. Numerical methods are very helpful when the differential equations of motion cannot be solved in a closed-form. Also, there are many numerical integration methods used to solve such equations of motion. The two main methods used for direct integration are: 1) explicit method, 2) implicit method. One of the methods used in the collection of implicit methods is the Wilson-Theta numerical integration method. Due to the accuracy and precision of the method and its high applicability used by previous researchers, this method is used in this paper to solve the final equations which will be described in following.

3 Wilson-Theta numerical integration method

The complete algorithm used in the Wilson-Theta method is showed in Fig. 2.

Fig. 2 shows the algorithm of the Wilson Theta numerical method [23–25] to solve the problem of dynamic train-track interaction. As can be seen in this method, first the stiffness, damping, and mass matrices of the whole system are calculated, and by estimating the initial values for displacement (X_0), velocity ($\dot{X}_0$), and acceleration ($\ddot{X}_0$) and selecting a specific time step (Δt), the constant coefficients (α_0 to α_8) of this method calculated. Then, by using these coefficients and within a loop and for the next time steps, the external load, acceleration ($\ddot{X}_{t+\theta\Delta t}$), velocity ($\dot{X}_{t+\theta\Delta t}$), and displacement ($X_{t+\theta\Delta t}$) matrices of the system are calculated.

4 Analysis algorithm of train–track dynamic problem

In the current study, four vertical moving loads are modeled on the rail by using finite element method. In this case, the length of the railway track is assumed to be 100.2 meters, including 167 beam elements with 0.6 meters long and also 168 nodes, that starting and ending nodes are considered to be the fixed joint supports in the modeling and considered sleeper is 0.6 m. In this situation, the vertical loads on the rail are introduced as vertical loads with a value of 100 kN. These moving loads run at a speed of 20 [m/s] (72 [km/h]) along the track. Fig. 3 shows the analysis algorithm of train – track dynamic interaction.

Fig. 3 shows how to perform and analyze for solving train–track dynamic problem by using finite element coding method. In this algorithm, first, the specifications of the railway track and the moving vehicle are given to the software as input data, and by using these data in the next step, the mass, stiffness, and damping matrices of these two parts had calculated. Also, the rail stiffness matrix had been calculated according to investigate the effects of a considering longitudinal force in the railway track. Then, the coding software is starting to obtain the dynamic responses by using an iteration loop that continues until the moving loads are on the railway track. The approach used for numerical simulation in this software is the Wilson-Theta method. In the continuation of the research, diagrams related to sensitivity analysis for changes in longitudinal forces and velocity had been presented. The various values of the track components and the different parameters of the moving vehicle in the ballasted-railway track system used in MATLAB coding are in Table 3 as follows: [26, 27]

5 Validation of the research results

This section presents a graph of numerical simulation results obtained using the Wilson-Theta method and compared with the results of Zakeri and Xia's [14] research on rail displacement.

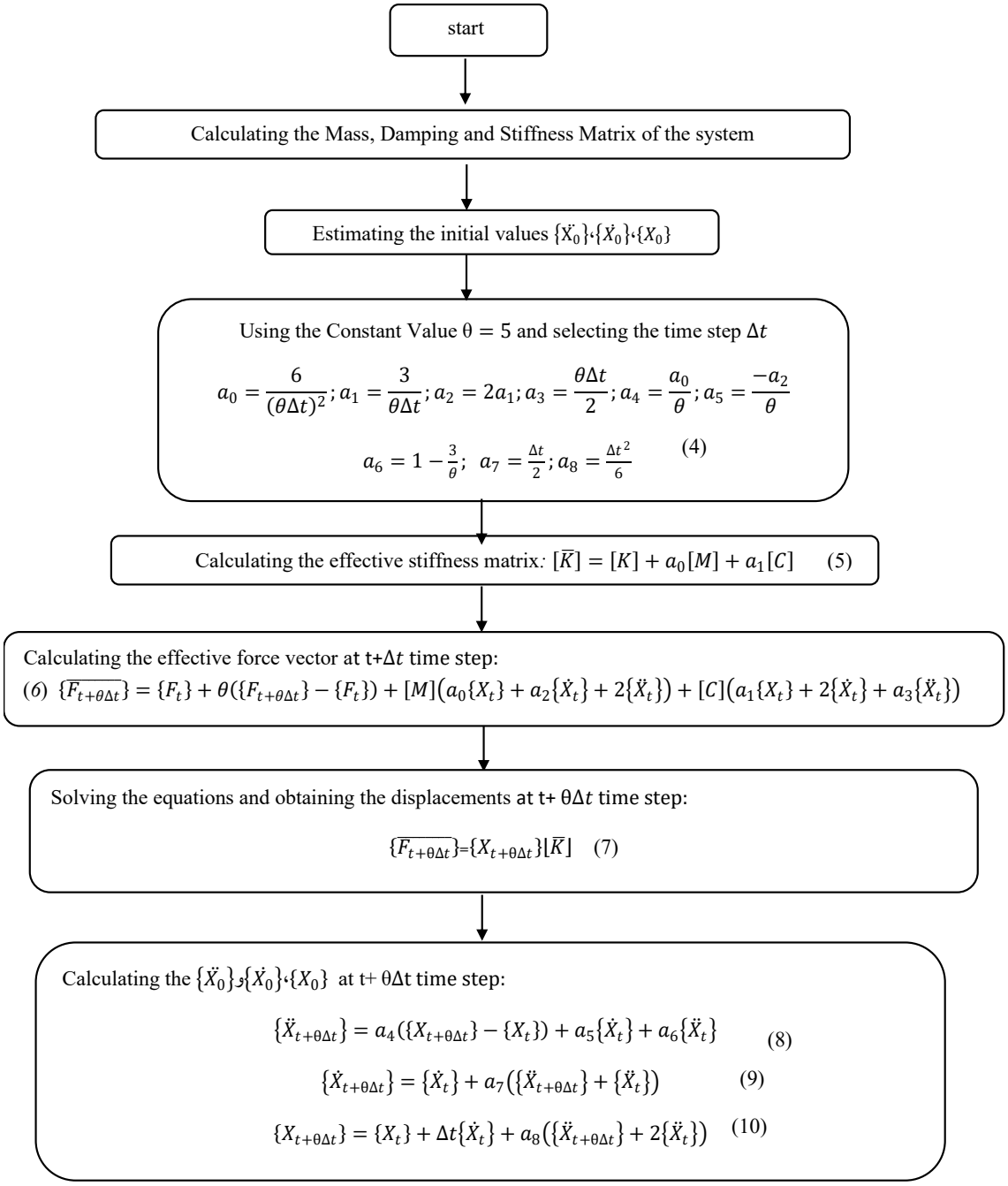

Fig. 2 The analysis algorithm of train–track dynamic interaction based on Wilson-Theta integration method [23–25]

As shown in the Fig 4. diagram, the results obtained through software simulation are in good accordance with the results of previous study on the rail displacement of four moving loads at a train speed of 20 [m/s].

6 Dynamic responses of train-track system

In this section, output results for rail displacement, sleeper velocity, ballast acceleration, at a speed of 20 [m/s] (72 [km/h]) and also a longitudinal force with the amount of 1500 [kN] are presented as follows:

Fig. 5(a) shows a chart of the vertical displacement changes of the rail according to the position of the moving loads on the railway track with and without applying a compressive and tensile axial force of 1500 [kN] at T = 2.5 seconds. As shown in Fig. 5(a), the maximum displacement of the rail that occurs in the middle of the railway track decreases by moving away from wheel loads. Fig. 5(b) shows a peak values of sleeper velocity chart according to the position of the moving loads on the railway track with and without applying a compressive and tensile axial

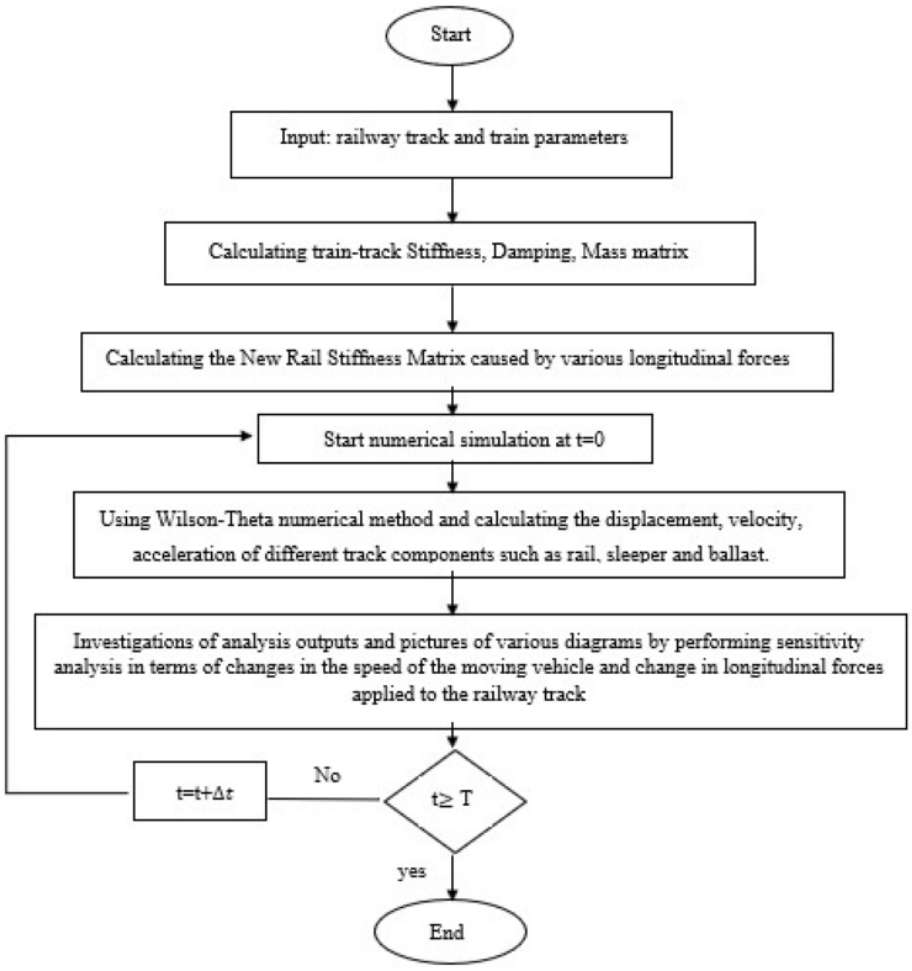

Fig. 3 The algorithm for how to use MATLAB software

force of 1500 [kN] at T = 2.5 seconds. As shown in Fig. 5(b), the maximum velocity of the sleeper that occurs in the middle of the railway track decreases by moving away from wheel loads.

Fig. 6 shows a peak values of ballast acceleration chart according to the position of the moving loads on the railway track with and without applying a compressive and tensile axial force of 1500 [kN] at T = 2.5 seconds. As shown in Fig. 6, the maximum acceleration of the ballast that occurs in the middle of the railway track decreases by moving away from wheel loads.

7 Sensitivity analysis on the train-track parameters

The tensile and compressive longitudinal forces with different values are applied to the railway track system, and also the train speed is changed simultaneously, which results on the different parameters are as follows:

Fig. 7(a) and 7(b) are related to the velocity, displacement of the rails, respectively. As can be seen, increasing the speed of the train and the longitudinal force increases these values for rail. Fig. 7(a) and 7(b) shows maximum rail velocity and displacement in the application of different longitudinal forces and train speeds for the first wheel load, in the state of applying four moving loads.

Fig. 8(a) and 8(b) are related to the rail acceleration and sleeper velocity, respectively. Fig. 8(a) shows maximum rail acceleration in the application of different longitudinal forces and train speeds for the first and second wheel load, in the state of applying four moving loads. Fig. 8(b) demonstrates maximum sleeper velocity in the application of different longitudinal forces and various train speeds for the first wheel load, in the state of applying four moving loads.

Fig. 9(a) shows maximum sleeper acceleration in the application of different longitudinal forces and various train speeds for the first wheel load, in the state of applying four moving loads. Fig. 9(b) displays maximum ballast velocity in the application of different longitudinal forces and train speeds for the second wheel load, in the state of applying four moving loads.

Table 3 Various values of the track components and vehicle model [26, 27]

Description	Value	Unit
Rail modulus of elasticity	206	GPa
Rail profile moment of inertia	32,200,000	mm^4
Rail mass per unit length	60	kg/m
Sleeper mass	320	kg
Ballast stiffness	70,000	kN/m
Ballast mass	1400	kg
Ballast density	1800	kg/m^3
Ballast thickness	30	cm
Rail pad stiffness	240,000	kN/m
Rail pad damping	248	kN.s/m
Subgrade stiffness	130	kN/m
Subgrade damping	62.3	kN.s/m
Car body mass	49,500	kg
Car body polar moment of inertia	1,700,000	$kg.m^2$
Car body length	15.06	m
Car body width	2.095	m
Bogie mass	10,750	kg
Bogie polar moment of inertia	9600	$kg.m^2$
Bogie length	4.2	m
Bogie width	2.095	m
Bogie height	1.15	m
Gravity acceleration (g)	10	m/s^2
Wheel mass	2200	kg
Wheel radius	0.46	m
Train speed	10 to 100	m/s
Train speed	36 to 360	km/h
Halves of wheels axles	1.5	m
Halves of bogies axles	7	m
Primary suspension system stiffness	4360	kN/m
Primary suspension system damping	220	kN.s/m
Secondary suspension system stiffnessv	1720	kN/m
Secondary suspension system vertical damping	300	kN.s/m

Fig. 10 expresses comparison diagram of the maximum displacement of the rail in the state of applying four moving loads for the first- and second wheel loads considering longitudinal force simultaneously with different values. The diagrams in Figs. 7 to 10 show the effect of increasing the axial (longitudinal) force and speed of the train on the maximum values of displacement, velocity, acceleration of different railway track components. Train speeds of 10, 20, 50, and 100 meters per second (36, 72, 180 and 360 [km/h]) assumed in this study, and the range of changes in longitudinal force is from –2000 [kN] to 2000 [kN]. A negative force indicates a longitudinal tensile force, and a positive

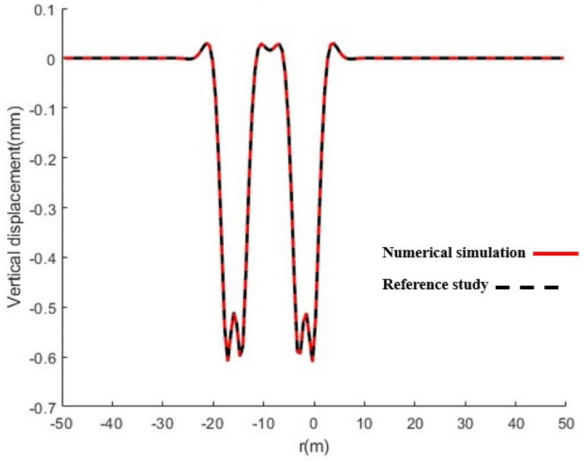

Fig. 4 Validation results of current and reference study

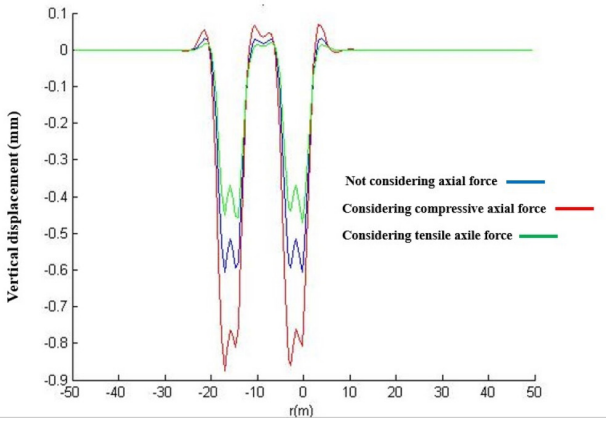

(a)

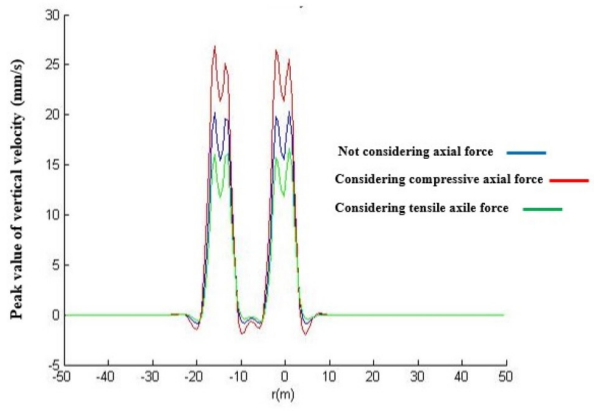

(b)

Fig. 5 Output results for rail displacement, sleeper velocity with and without applying compressive and tensile longitudinal force with the value of 1500 [kN] at T = 2.5 [s]

one shows the compressive longitudinal forces. Also, increasing the speed of the train from 10 [m/s] (36 [km/h]) to 100 [m/s] (360 [km/h]) and increasing a longitudinal force from –2000 [kN] of tensile to 2000 [kN] of compressive increases the velocity and acceleration of the sleeper in Figs. 8(b) and 9(a) and also ballast velocity in Fig. 9(b).

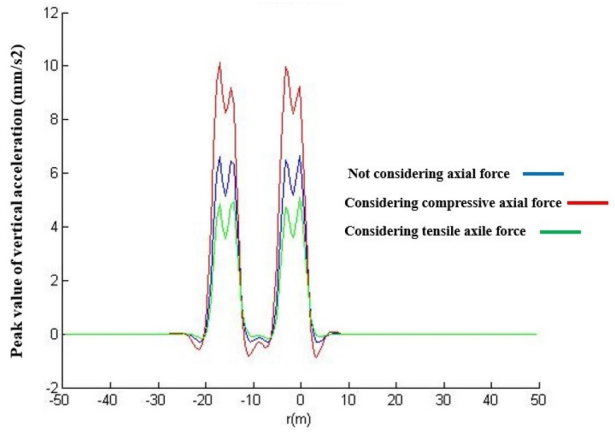

Fig. 6 Output results for ballast acceleration with and without applying compressive and tensile longitudinal force with the value of 1500 [kN] at T = 2.5 [s]. * Note: r(m)= The wheel position of the moving train along the railway track

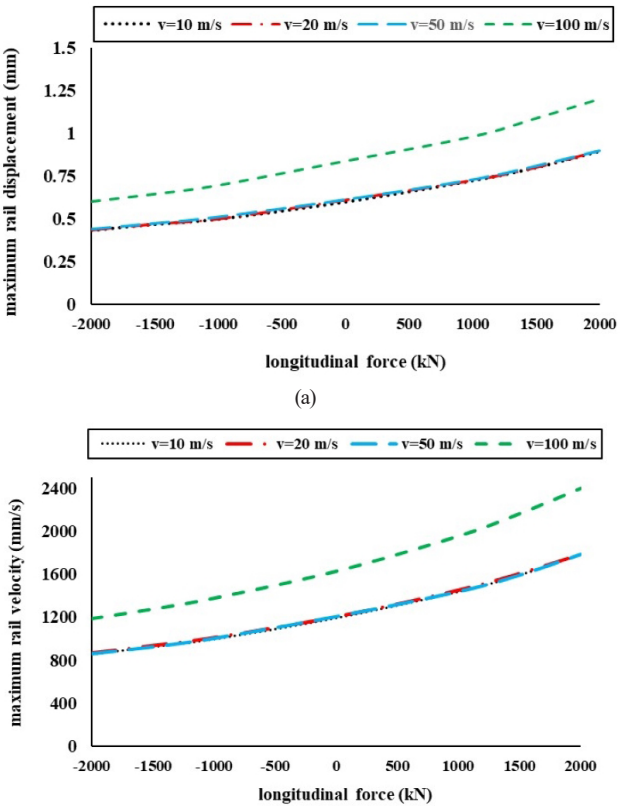

Fig. 7 Diagrams of maximum rail velocity and displacement in the application of different longitudinal forces and train speeds

8 Conclusions

In the present study, the dynamic train – track interaction problem was simulated by using the finite element and Wilson-Theta numerical integration method focused on the effects of longitudinal forces for vertical moving loads with the value of 100 [kN]. The results are presented for

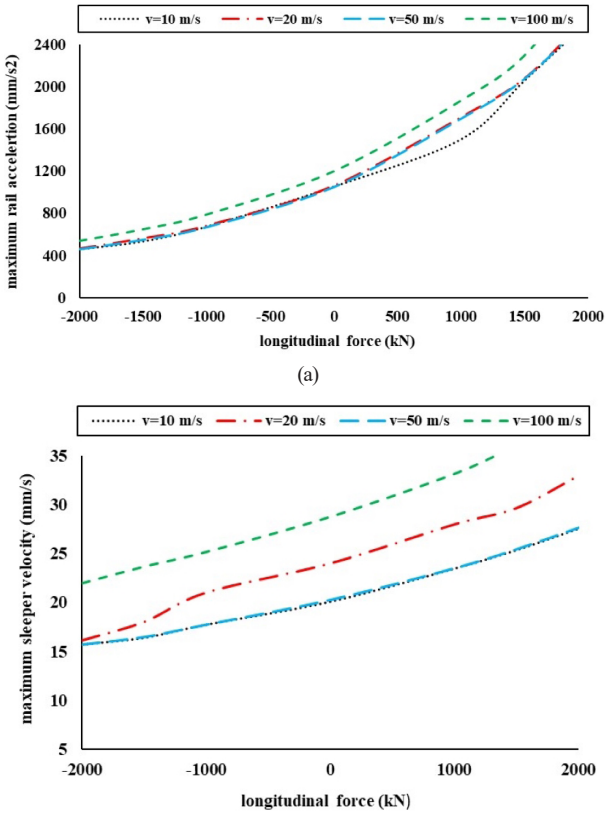

Fig. 8 Diagrams of maximum rail acceleration and sleeper velocity in the application of different longitudinal forces and train speeds

different railway track components such as rail, sleeper, ballast layers. Also, by sensitivity analysis for changing the longitudinal forces from –2000 [kN] to 2000 [kN] and for different train speeds from 10 [m/s] (36 [km/h]) to 100 [m/s] (360 [km/h]) applied to the railway track, the effects of these factors on the different parameters like displacement, velocity and acceleration were presented and important results are summarized as follows:

- The values of rail displacement increase significantly by 33 percent when both the compressive force and the vertical moving loads are applied to the track simultaneously compared with the state of just considering vertical moving loads.
- The values of rail displacement decrease by 25% when the tensile force and the vertical moving loads are applied to the track simultaneously in comparison with the case of not applying them.
- The values of sleeper velocity increase by 25.9% when the compressive force and the vertical moving loads are applied to the track simultaneously compared with the state of just considering vertical moving loads.

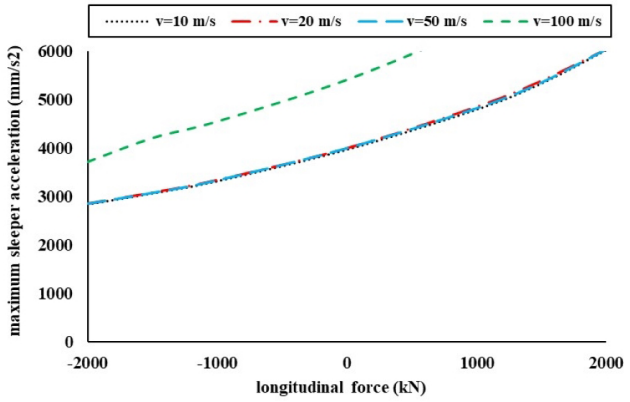

(a)

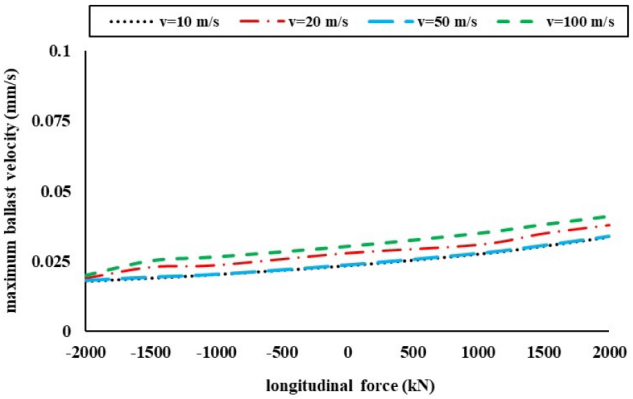

(b)

Fig. 9 Diagrams of sensitivity analysis results on sleeper acceleration and ballast velocity in the application of different longitudinal forces and various train speeds

- The values of sleeper velocity decrease by 15% when the tensile force and the vertical moving loads are applied to the track simultaneously compared with the state of just considering vertical moving loads.
- The values of ballast acceleration increase by 27.7% when the compressive force and the vertical moving loads are applied to the track simultaneously compared with the state of just considering vertical moving loads.
- The values of ballast acceleration reduce by 20% when the tensile force and the vertical moving loads are applied to the track simultaneously compared with the state of just considering vertical moving loads.
- The displacement of the rail increases by 27.12%, 26.40%, and 27%, respectively, by increasing the speed of the train from 10 [m/s] (36 [km/h]) to 100 [m/s] (360 [km/h]) in all three modes without applying axial force, considering compressive and tensile one (1500 [kN]), respectively. (For the first wheel load in the state considering several moving loads).
- The velocity of the rail increases by 25.9%, 25.6%, and 36.25%, respectively, by increasing the speed of the train from 10 [m/s] (36 [km/h]) to 100 [m/s] (360 [km/h]) in all three modes without applying axial force, considering compressive and tensile one (1500 [kN]), respectively. (For the first wheel load in the state considering several moving loads).

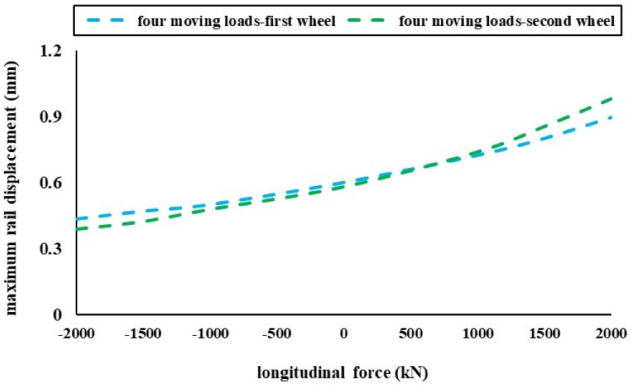

Fig. 10 Comparison diagram of the maximum displacement of the rail in the state of applying four moving loads for the first- and second wheel loads considering longitudinal force simultaneously with different values

- The acceleration of the rail increases by 11.6%, 9.56%, and 13.84%, respectively, by increasing the speed of the train from 10 [m/s] (36 [km/h]) to 100 [m/s] (360 [km/h]) in all three modes without applying axial force, considering compressive and tensile one (1500 [kN]), respectively. (For the first wheel load in the state considering several moving loads).
- The velocity of the sleeper increases by 29.5%, 28%, and 24%, respectively, by increasing the speed of the train from 10 [m/s] (36 [km/h]) to 100 [m/s] (360 [km/h]) in all three modes without applying axial force, considering compressive and tensile one (1500 [kN]), respectively. (For the first wheel load in the state considering several moving loads).
- The acceleration of the sleeper increases by 26.03% and 26.6%, respectively, by increasing the speed of the train from 10 [m/s] (36 [km/h]) to 100 [m/s] (360 [km/h]) in all three modes without applying axial force and considering tensile force (1500 [kN]), respectively. (For the first wheel load in the state considering several moving loads).
- The velocity of the ballast increases by 7.7%, 7.8%, and 9%, respectively, by increasing the speed of the train from 10 [m/s] (36 [km/h]) to 100 [m/s] (360 [km/h]) in all three modes without applying axial force, considering compressive and tensile one (1500 [kN]), respectively. (For the second wheel load in the state considering several moving loads).

The dynamic responses of the train-track system (displacement, acceleration and velocity) for rail, sleeper and ballast increase if the railway track contains geometrical faults in all three modes of considering compressive force (**C**), Tensile force (*T*) and just train vertical moving loads. "Investigations on the Effects of Rail Longitudinal Forces in Train-Track Dynamic Interaction including track geometrical faults "is one of the future research possibilities for the authors and also maybe for other researchers in this area to obtain the exact effects of these faults on railway track and train safety indices.

Declaration of conflicting interest
The author(s) declared no potential conflicts of interest with respect to the research, authorship, and/or publication of this article.

Funding Statement
The author(s) received no financial support for the research, authorship, and/or publication of this article.

References

[1] Taghipour, A., Zakeri, J. A., Jahangiri, M., Mosayebi, S. A. "Investigating the dynamic behaviour of a railway bridge subjected to over-height vehicle collision", Australian Journal of Structural Engineering, 24(3), pp. 217–227, 2023. https://doi.org/10.1080/13287982.2023.2176972

[2] Mosayebi, S.-A., Zakeri, J.-A., Esmaeili, M. "Vehicle/track dynamic interaction considering developed railway substructure models", Structural Engineering and Mechanics, 61(6), pp. 775–784, 2017. https://doi.org/10.12989/sem.2017.61.6.775

[3] Mosayebi, S.-A., Zakeri, J.-A., Esmaeili, M. "A comparison between the dynamic and static stiffness of ballasted track", Geomechanics and Engineering, 11(6), pp. 757–776, 2016. https://doi.org/10.12989/gae.2016.11.6.757

[4] Lei, X., Zhai, W. "A three-dimensional dynamic model for train-track interactions", Applied Mathematical Modelling, 76(1), pp. 443–465, 2019. https://doi.org/10.1016/j.apm.2019.04.037

[5] Xu, Y., Yang, C., Zhang, W., Zhu, W., Fan, W., Mei, G., Mou, J. "Study on the influence of lateral and local rail deformation on the train–track interaction dynamics", Vehicle System Dynamics, 60(2), pp. 670–698, 2020. https://doi.org/10.1080/00423114.2020.1828596

[6] Nishiura, D., Sakai, H., Aikawa, A., Tsuzuki, S., Sakaguchi, H. "Novel discrete element modeling coupled with finite element method for investigating ballasted railway track dynamics", Computers and Geotechnics, 96(1), pp. 40–54, 2017. https://doi.org/10.1016/j.compgeo.2017.10.011

[7] Shih, J. Y., Thompson, D. J., Zervos, A. "The effect of boundary conditions, model size and damping models in the finite element modelling of a moving load on a track/ground system", Soil Dynamics and Earthquake Engineering, 89, pp. 12–27, 2016. https://doi.org/10.1016/j.soildyn.2016.07.004

[8] Mosayebi, S.-A., Zakeri, J.-A., Esmaeili, M. "Field test investigation and numerical analysis of ballasted track under moving locomotive", Journal of Mechanical Science and Technology, 30, pp. 1065–1069, 2017. https://doi.org/10.1007/s12206-016-0209-3

[9] Mosayebi, S.-A., Zakeri, J.-A., Esmaili, M. "Some Aspects of Support Stiffness Effects on Dynamic Ballasted Railway Tracks", Periodica Polytechnica Civil Engineering, 60(3), pp. 427–436, 2016. https://doi.org/10.3311/PPci.7933

[10] Czyczula, W., Koziol, P., Kudla, D., Lisowski, S. "Analytical evaluation of track response in the vertical direction due to a moving load", Journal of Vibration and Control, 23(18), pp. 2989–3006, 2017. https://doi.org/10.1177/1077546315625823

[11] Hou, K., Kalousek, R., Dong, R. "Dynamic model for an asymmetrical vehicle/track system", Journal of Sound and Vibration, 267(3), pp. 591–604, 2003. https://doi.org/10.1016/S0022-460X(03)00726-0

[12] Zhai, W., Sun, X. "A Detailed Model for Investigating Vertical Interaction between Railway Vehicle and Track", Vehicle System Dynamics, 23(1), pp. 603–615, 1994. https://doi.org/10.1080/00423119308969544

[13] Wang, Q, Xiao, X.-B., Wang, J.-N., Wang, W., Yang, Y., Jin, X.-S. "Train/track coupled dynamics model of long heavy haul train based on substructure and parallel computing", Proceedings of the Institution of Mechanical Engineers, Part F: Journal of Rail and Rapid Transit, 2023. https://doi.org/10.1177/09544097231196338

[14] Zakeri, J. A., Xia, H. "Sensitivity analysis of track parameters on train-track dynamic interaction", Journal of Mechanical Science and Technology, 22(7), pp. 1299–1304, 2008. https://doi.org/10.1007/s12206-008-0316-x

[15] Zakeri, J. A., Fattahi, M., Nouri, M., Janatabadi, F. "Influence of Rail Pad Stiffness and Axle Loads on Dynamic Responses of Train-track Interaction with Unsupported Sleepers", Periodica Polytechnica Civil Engineering, 64(2), pp. 524–534, 2020. https://doi.org/10.3311/PPci.14826

[16] Alkaissi, Z. A. "Three Dimensional Finite Element Model of Railway Ballasted Track System under Dynamic Train Loading", Construction Technologies and Architecture, 8, pp. 11–21, 2023. https://doi.org/10.4028/p-6X6HPi

[17] Liu, Z., Feng, B., Tutumluer, E. "Coupling Train-Track Models with the Discrete Element Method for a More Realistic Simulation of Ballasted Track Dynamic Behavior", Transportation Research Record, 2677(8), pp. 414–427, 2023. https://doi.org/10.1177/03611981231156933

[18] The MathWorks Inc. "MATLAB toolbox version 9.13.0 (R2022b)", [online] Available at: https://www.mathworks.com/products

[19] Jiang, L., Feng, Y., Zhou, W., He, B. "Vibration characteristic analysis of high-speed railway simply supported beam bridge-track structure system", Steel and Composite Structures, 31(6), pp. 591–600, 2019.
https://doi.org/10.12989/scs.2019.31.6.591

[20] Taghipour, A., Zakeri, J. A., Mosayebi, S. A. "Investigating the thermal force effect of the rail on dynamic analysis of railway track under dynamic load", Quarterly Journal of Transportation Engineering, 13(1), pp. 1149–1162, 2021.
https://doi.org/10.22119/jte.2020.115215

[21] Mosayebi, S.-A. Esmaeili, M., Zakeri, J.-A. "Numerical investigation of the effects of unsupported railway sleepers on train-induced environmental vibrations", Journal of Low Frequency Noise, Vibration and Active Control, 36(2), pp. 160–176, 2017.
https://doi.org/10.1177/026309231771199

[22] Zakeri, J.-A., Esmaeili, M., Mosayebi, S.-A. "Effects of sleeper support modulus on dynamic behaviour of railway tracks caused by moving wagon", International Journal of Heavy Vehicle Systems, 24(3), pp. 277–287, 2017.
https://doi.org/10.1504/IJHVS.2017.084852

[23] Ahlbeck, D. R., Meacham, H. C., Prause, R. H. "The development of analytical models for railroad track dynamics", In: Kerr, A. D. (ed.) Railroad Track Mechanics and Technology, Pergamon, 1978, pp. 239–263. ISBN 978-0-08-021923-3
https://doi.org/10.1016/B978-0-08-021923-3.50017-6

[24] Craig Jr., R. R., Kurdila, A. J. "Fundamentals of Structural Dynamics", John Wiley & Sons, 2011. ISBN 0471430447

[25] Davis, P. J., Rabinowitz, P. "Methods of numerical integration: Second edition", Dover Publications, 2007. ISBN 0486453391

[26] Mosayebi, S.-A., Zakeri, J.-A., Esmaeili, M. "Effects of train bogie patterns on the mechanical performance of ballasted railway tracks with unsupported", Proceedings of the Institution of Mechanical Engineers, Part F: Journal of Rail and Rapid Transit, 232(1), pp. 238–248, 2018.
https://doi.org/10.1177/0954409716664932

[27] Mosayebi, S. A., Zakeri, J. A., Esmaeili, M. "Dynamic Train–Track Interactions and Stress Distribution Patterns in Ballasted Track Layers", Journal of Transportation Engineering, Part B: Pavements, 146(1), 04019042, 2020.
https://doi.org/10.1061/JPEODX.0000140